Comparing three approaches to the inducing source setting for the ground electromagnetic field modeling due to space weather events

Elena Marshalko[1], Mikhail Kruglyakov[1], Alexey Kuvshinov[2], Liisa Juusola[3], Norah Kaggwa Kwagala[4], Elena Sokolova[5], and Vyacheslav A. Pilipenko[6]

[1]Institute of Geophysics, ETH Zurich
[2]Institute of Geophysics
[3]Finnish Meteorological Institute
[4]University of Bergen
[5]Schmidt Institute of Physics of the Earth
[6]Space Research Institute

November 24, 2022

Abstract

Ground-based technological systems, such as power grids, can be affected by geomagnetically induced currents (GIC) during geomagnetic storms and magnetospheric substorms. This motivates the necessity to numerically simulate and, ultimately, forecast GIC. The prerequisite for the GIC modeling in the region of interest is the simulation of the ground geoelectric field (GEF) in the same region. The modeling of the GEF in its turn requires spatio-temporal specification of the source which generates the GEF, as well as an adequate regional model of the Earth's electrical conductivity. In this paper we compare results of the GEF (and ground magnetic field) simulations using three different source models. Two models represent the source as a laterally varying sheet current flowing above the Earth. The first model is constructed using the results of a physics-based 3-D magnetohydrodynamic (MHD) simulation of near-Earth space, the second one uses ground-based magnetometers' data and the Spherical Elementary Current Systems (SECS) method. The third model is based on a "plane wave" approximation which assumes that the source is locally laterally uniform. Fennoscandia is chosen as a study region and the simulations are performed for the 7-8 September 2017 geomagnetic storm. We conclude that ground magnetic field perturbations are reproduced more accurately using the source constructed via the SECS method compared to the source obtained on the basis of MHD simulation outputs. We also show that the difference between the GEF modeled using laterally nonuniform source and plane wave approximation is substantial in Fennoscandia.

Comparing three approaches to the inducing source setting for the ground electromagnetic field modeling due to space weather events

Elena Marshalko[1,2,3], Mikhail Kruglyakov[1,4], Alexey Kuvshinov[1], Liisa Juusola[5], Norah Kaggwa Kwagala[6], Elena Sokolova[2], Viacheslav Pilipenko[2,3]

[1]Institute of Geophysics, ETH Zürich, Zürich, Switzerland
[2]Institute of Physics of the Earth, Moscow, Russia
[3]Geophysical Center, Moscow, Russia
[4]Geoelectromagnetic Research Center, Institute of Physics of the Earth, Moscow, Russia
[5]Finnish Meteorological Institute, Helsinki, Finland
[6]Space Plasma Physics Group, Department of Physics and Technology, University of Bergen, Bergen, Norway

Key Points:

- 3-D electromagnetic field modeling is performed for Fennoscandia exploiting three different inducing source models
- Magnetic field perturbations are reproduced much more accurately using the SECS source than using the source based on MHD simulation outputs
- The difference between geoelectric fields modeled using laterally nonuniform source and plane wave approach is substantial in Fennoscandia

Corresponding author: Elena Marshalko, elena.e.marshalko@gmail.com

Abstract

Ground-based technological systems, such as power grids, can be affected by geomagnetically induced currents (GIC) during geomagnetic storms and magnetospheric substorms. This motivates the necessity to numerically simulate and, ultimately, forecast GIC. The prerequisite for the GIC modeling in the region of interest is the simulation of the ground geoelectric field (GEF) in the same region. The modeling of the GEF in its turn requires spatio-temporal specification of the source which generates the GEF, as well as an adequate regional model of the Earth's electrical conductivity. In this paper we compare results of the GEF (and ground magnetic field) simulations using three different source models. Two models represent the source as a laterally varying sheet current flowing above the Earth. The first model is constructed using the results of a physics-based 3-D magnetohydrodynamic (MHD) simulation of near-Earth space, the second one uses ground-based magnetometers' data and the Spherical Elementary Current Systems (SECS) method. The third model is based on a "plane wave" approximation which assumes that the source is locally laterally uniform. Fennoscandia is chosen as a study region and the simulations are performed for the 7-8 September 2017 geomagnetic storm. We conclude that ground magnetic field perturbations are reproduced more accurately using the source constructed via the SECS method compared to the source obtained on the basis of MHD simulation outputs. We also show that the difference between the GEF modeled using laterally nonuniform source and plane wave approximation is substantial in Fennoscandia.

1 Introduction

Large coronal mass ejections from the Sun release massive amounts of plasma, which flow at high speed into the interplanetary space. The interaction of this solar wind with the Earth's magnetosphere can lead to significant spatio-temporal disturbances of the magnetic field at the surface of the Earth, which are known as geomagnetic storms. These space weather events induce a geoelectric field (GEF) in the Earth's subsurface, which in turn drives geomagnetically induced currents (GIC) in ground-based technological systems such as power grids and pipelines posing a significant risk to the reliability and durability of such infrastructure.

The core component in quantitative estimation of the hazard to technological systems from space weather is as realistic as practicable numerical modeling of GIC, and, ultimately, their forecasting. Ideally, to perform GIC modeling one needs the following ingredients: a) a realistic model of the source of geomagnetic disturbances; b) a comprehensive three-dimensional (3-D) electrical conductivity model of the Earth's subsurface in the region of interest; c) a 3-D numerical solver which allows for accurate and detailed modeling of the GEF in a given conductivity model excited by a given source; d) the geometry of transmission lines and system design parameters that allow for the conversion of the modeled GEF into GIC.

Many previous studies in connection with GIC operated with simplified models either of conducting Earth (one-dimensional (1-D) or thin sheet conductivity models) or the source (vertically propagating laterally uniform electromagnetic (EM) field; plane wave), or both (e.g., Viljanen et al. (2012, 2013, 2014); Püthe and Kuvshinov (2013); Püthe et al. (2014); Beggan et al. (2013); Beggan (2015); Kelly et al. (2017); Honkonen et al. (2018); Bailey et al. (2017, 2018); Divett et al. (2017, 2020)).

In spite of the fact that the importance of performing simulations using fully 3-D conductivity models is currently widely recognised (Kelbert, 2020), such simulations are still rather rare in the GIC community (e.g., Wang et al. (2016); Pokhrel et al. (2018); Nakamura et al. (2018); Liu et al. (2018); Marshall et al. (2019); Rosenqvist and Hall (2019); Marshalko et al. (2020)), mostly due to the lack of the credible 3-D conductivity models of the regions of interest as well as unavailability of adequate tools to model the problem in the full complexity.

As for the source, approximating it by plane waves still prevails in the GIC-related studies (e.g., Kelbert et al. (2017); Kelbert and Lucas (2020); Lucas et al. (2018); Campanya et al. (2019); Sokolova et al. (2019); Wang et al. (2020)). This approximation seems reasonable in low and middle latitudes, where the main source of anomalous geomagnetic disturbances is a large-scale magnetospheric ring current. However, the plane wave assumption may not work in higher latitudes, where the main source of the disturbances is the auroral ionospheric current, which is extremely variable both in time and space, especially during periods of enhanced geomagnetic activity (Belakhovsky et al., 2019). Marshalko et al. (2020) provided some evidence for that by comparing ground EM fields modeled in the eastern United States using the plane wave approximation and the excitation by a laterally variable source which was constructed using outputs from 3-D magnetohydrodynamic (MHD) simulation of near-Earth space. The authors found that the difference increases towards higher latitudes where the lateral variability of the source expectedly enlarges. However their modeling was mostly confined to mid-latitude region, thus it is still unclear how pronounced the difference between the plane wave and "laterally varying source" results could be in auroral regions. In this paper we investigate this problem using Fennoscandia as a study region. The choice of Fennoscandia is motivated by: a) high-latitude location of the region; b) the availability of the 3-D ground electrical conductivity model of the region (Korja et al., 2002) c) the existence of the regional magnetometer network (International Monitor for Auroral Geomagnetic Effect, IMAGE (Tanskanen, 2009)) allowing us to build data-based model of a laterally variable source, which is a natural alternative to physics-based (MHD) source model in the areas with a reasonably dense net of observations.

Specifically, we perform 3-D modeling of ground electric and magnetic fields in Fennoscandia using three different source models and taking 7–8 September 2017 geomagnetic storm as a space weather event. Two models approximate the source by laterally varying sheet current flowing above the Earth's surface. One of the models is built using the results of physics-based 3-D MHD simulation of the near-Earth space, another model uses the IMAGE magnetometer data and the Spherical Elementary Current Systems (SECS) method (Vanhamäki & Juusola, 2020; Juusola et al., 2020). The third modeling is based on a "plane wave" approximation which assumes that the source is locally laterally uniform. Note that previous GIC-related studies in Fennoscandia operated with both 1-D (e.g., Pulkkinen et al. (2005); Myllys et al. (2014); Viljanen and Pirjola (2017)) and 3-D (Rosenqvist & Hall, 2019; Dimmock et al., 2019, 2020) Earth's conductivity models, the magnetic field in most of these papers was allowed to be laterally variable, but the GEF was always calculated implicitly assuming the plane wave excitation.

We compare modeling results and discuss found differences and similarities. We also compare results of magnetic field modeling with observations. The paper is organized as follows. The methodology used is described in Section 2.1 followed by presentation of our results in Section 3. Finally, the discussion of our results and conclusions are given in Section 4.

2 Methodology

2.1 Governing equations and modeling scheme

We compute the electric, $\mathbf{E}(t,\mathbf{r})$, and magnetic, $\mathbf{B}(t,\mathbf{r})$, fields for a given Earth's conductivity distribution $\sigma(\mathbf{r})$ and a given inducing source $\mathbf{j}^{ext}(t,\mathbf{r})$, where t and $\mathbf{r} = (x,y,z)$ denote time and position vector, correspondingly. These fields obey Maxwell's equations, that are written in the time domain as

$$\frac{1}{\mu_0}\nabla \times \mathbf{B} = \sigma\mathbf{E} + \mathbf{j}^{ext}, \tag{1}$$

$$\nabla \times \mathbf{E} = -\frac{\partial \mathbf{B}}{\partial t}, \tag{2}$$

where μ_0 is the magnetic permeability of a free space. Note that this formulation of Maxwell's equations neglects displacement currents, which are insignificant in the range of periods considered in this study. We solve eqs (1)-(2) numerically using the following three-step procedure:

1. The inducing source $\mathbf{j}^{ext}(t, \mathbf{r})$ is transformed from the time to the frequency domain with a fast Fourier transform (FFT).

2. Maxwell's equations in the frequency domain

$$\frac{1}{\mu_0}\nabla \times \mathbf{B} = \sigma\mathbf{E} + \mathbf{j}^{ext}, \tag{3}$$

$$\nabla \times \mathbf{E} = i\omega\mathbf{B}, \tag{4}$$

   are numerically solved for the corresponding angular frequencies $\omega = 2\pi f$, using the scalable 3-D EM forward modeling code PGIEM2G (Kruglyakov & Kuvshinov, 2018), based on a method of volume integral equations (IE) with a contracting kernel (Pankratov & Kuvshinov, 2016).

   We would like to note here that in our previous papers (Ivannikova et al., 2018; Marshalko et al., 2020) we used modeling code *extrEMe* (Kruglyakov et al., 2016) which is also based on IE method. The distinction between two codes lies in different piece-wise bases used. PGIEM2G exploits a piece-wise polynomial basis whereas *extrEMe* uses a piece-wise constant basis. We found that in order to properly account for the effects (in electric field) from extremely large conductivity contrasts in the Fennoscandian region, *extrEMe* requires significantly larger computational loads compared to the PGIEM2G. This is the reason why we used the PGIEM2G code rather than *extrEMe* to obtain modeling results presented in this paper. Specifically, PGIEM2G was run with the use of first-order polynomials in lateral directions and third-order polynomials in the vertical direction.

   Frequencies f range between $\frac{1}{L}$ and $\frac{1}{2\Delta t}$ where L is the length of the (input) times series of the inducing current $\mathbf{j}^{ext}(t, \mathbf{r})$, and Δt is the sampling rate of this time series. In this study Δt is 1 min, and L is 8 h.

3. $\mathbf{E}(t, \mathbf{r})$ and $\mathbf{B}(t, \mathbf{r})$ are obtained with an inverse FFT of the frequency-domain fields.

2.2 3-D conductivity model

3-D conductivity model of the region was constructed using the SMAP (Korja et al., 2002) – a set of maps of crustal conductances (vertically integrated electrical conductivities) of the Fennoscandian Shield, surrounding seas, and continental areas. The SMAP consists of six layers of laterally variable conductance. Each layer has the thickness of 10 km. The first layer comprises contributions from the sea water, sediments, and upper crust. The other five layers describe conductivity distribution in the middle and lower crust. SMAP covers an area 0°E – 50°E and 50°N – 85°N and has $5' \times 5'$ resolution. We converted the original SMAP database into Cartesian 3-D conductivity model of Fennoscandia with three layers of laterally variable conductivity of 10, 20 and 30 km thicknesses (Figures 1.a-c). This vertical discretization is chosen to be compatible with that previously used by Rosenqvist and Hall (2019) and Dimmock et al. (2019, 2020) for

GIC studies in the region. To obtain the conductivities in Cartesian coordinates we applied the transverse Mercator map projection (latitude and longitude of the true origin are 50°N and 25°E, correspondingly) to original data and interpolated the results onto a regular lateral grid. The lateral discretization and size of the resulting conductivity model were taken as 5×5 km^2 and 2550×2550 km^2, respectively. Deeper than 60 km we used a 1-D conductivity profile obtained by Grayver et al. (2017) (cf. Figure 1.d).

Figure 1. Conductivity distribution [S/m] in the model: a)–c) Plane view on 3 layers of the 3-D part of the model; d) global 1-D conductivity profile derived by Grayver et al. (2017) and used in this study. Locations of geomagnetic observatories Abisko (ABK), Uppsala (UPS), Saint Petersburg (SPG), and P1, P2 and P3 points are marked with circles in plot (a).

2.3 EM induction source settings

In this section we discuss the construction of two models for laterally variable source and also explain how EM field is calculated in the framework of plane wave (laterally uniform source) concept. The sources are set up for the geomagnetic storm on 7-8 Septem-

Figure 2. Global snapshots of the external magnetic eld components at the surface of the Earth computed based on the SWMF outputs at 23:16 and 23:52 UT on 7 September 2017. B_x, B_y and B_z are northward, eastward and downward directed components, respectively.

2.3.2 Construction of the source using the SECS method

The second model of the source was constructed using the SECS method (Vanhamäki & Juusola, 2020). In this method the elementary current systems form a set of basis functions for representing two-dimensional vector elds on a spherical surface. An important application of the SECS method, which is relevant for this study, is the estimation of the ionospheric current system from ground-based measurements of magnetic eld distur-

Figure 5. The same legend as in Figure 4 but for Uppsala (UPS) geomagnetic observatory.

Finally, two lower plots in Figures 4 - 6 show plane-wave-, SECS- and MHD-based horizontal GEF. Note that long-term continuous observations of GEF are absent in the region, thus only modeling results are shown in the plots.

Similarly to MHD-based magnetic field, the MHD-based GEF is underestimated compared to the SECS-based GEF. The correlation between these modeling results is very low and nRMSE are high (see Table 3).

On the contrary, SECS- and plane wave-based electric fields are rather close to each other, especially at locations of UPS and SPG observatories; Table 4 illustrates this quantitatively. Correlation between modeling results at ABK observatory is lower and nRMSE is higher most likely due to the fact that this observatory is situated in the region with high lateral conductivity contrasts (resistive landmass and conductive sea). To put more weight on this inference last three columns of Table 4 and Figure 7 demonstrate SECS- and plane-wave-based results for three "sites" also located in the regions with high lat-

netically induced currents around New Zealand to explore GIC in the South Island's electrical transmission network. *Space Weather*, 15(10), 1396–1412. doi: 10.1002/2017SW001697

Divett, T., Mac Manus, D. H., Richardson, G. S., Beggan, C. D., Rodger, C. J., Ingham, M., . . . Obana, Y. (2020). Geomagnetically induced current model validation from New Zealand's South Island. *Space Weather*, 18(8), e2020SW002494. doi: 10.1029/2020SW002494

Grayver, A. V., Munch, F. D., Kuvshinov, A. V., Khan, A., Sabaka, T. J., & Tøffner-Clausen, L. (2017). Joint inversion of satellite-detected tidal and magnetospheric signals constrains electrical conductivity and water content of the upper mantle and transition zone. *Geophys. Res. Lett.*, 44(12), 6074–6081. doi: 10.1002/2017GL073446

Honkonen, I., Kuvshinov, A., Rastätter, L., & Pulkkinen, A. (2018). Predicting global ground geoelectric field with coupled geospace and three-dimensional geomagnetic induction models. *Space Weather*, 16(8), 1028–1041. doi: 10.1029/2018SW001859

Ivannikova, E., Kruglyakov, M., Kuvshinov, A., Rastätter, L., & Pulkkinen, A. (2018). Regional 3-D modeling of ground electromagnetic field due to realistic geomagnetic disturbances. *Space Weather*, 16(5), 476–500. doi: 10.1002/2017SW001793

Juusola, L., Vanhamäki, H., Viljanen, A., & Smirnov, M. (2020). Induced currents due to 3D ground conductivity play a major role in the interpretation of geomagnetic variations. *Ann. Geophys.*, 38(5), 983–998. doi: 10.5194/angeo-38-983-2020

Kelbert, A. (2020). The role of global/regional Earth conductivity models in natural geomagnetic hazard mitigation. *Surv. Geophys.*, 41, 115–166. doi: 10.1007/s10712-019-09579-z

Kelbert, A., Balch, C., Pulkkinen, A., Egbert, G., Love, J., Rigler, J., & Fujii, I. (2017). Methodology for time-domain estimation of storm time geoelectric fields using the 3-D magnetotelluric response tensors. *Space Weather*, 15(7), 874–894. doi: doi:10.1002/2017SW001594

Kelbert, A., & Lucas, G. M. (2020). Modified GIC estimation using 3-D Earth conductivity. *Space Weather*, 18(8), e2020SW002467. doi: 10.1029/2020SW002467

Kelly, G. S., Viljanen, A., Beggan, C. D., & Thomson, A. W. P. (2017). Understanding GIC in the UK and French high-voltage transmission systems during severe magnetic storms. *Space Weather*, 15(1), 99–114. doi: 10.1002/2016SW001469

Korja, T., Engels, M., Zhamaletdinov, A. A., Kovtun, A. A., Palshin, N. A., Smirnov, M. Y., . . . BEAR Working Group (2002). Crustal conductivity in Fennoscandia – a compilation of a database on crustal conductance in the Fennoscandian Shield. *Earth Planets Space*, 54, 535–558. doi: 10.1186/BF03353044

Kruglyakov, M., Geraskin, A., & Kuvshinov, A. (2016). Novel accurate and scalable 3-D MT forward solver based on a contracting integral equation method. *Computers and Geosciences*, 96, 208–217. doi: 10.1016/j.cageo.2016.08.017

Kruglyakov, M., & Kuvshinov, A. (2018). Using high-order polynomial basis in 3-D EM forward modeling based on volume integral equation method. *Geophys. J. Int.*, 213(2), 1387–1401. doi: 10.1093/gji/ggy059

Kwagala, N. K., Hesse, M., Moretto, T., Tenfjord, P., Norgren, C., Toth, G., . . . Spinnangr, S. F. (2020). Validating the Space Weather Modeling Framework (SWMF) for applications in northern Europe - Ground magnetic perturbation validation. *J. Space Weather Space Clim.*, 10, 33. doi: 10.1051/swsc/2020034

Linty, N., Minetto, A., Dovis, F., & Spogli, L. (2018). Effects of phase scintillation on the GNSS positioning error during the September 2017 storm at Svalbard.

Space Weather, *16*(9), 1317–1329. doi: 10.1029/2018SW001940

Liu, C., Wang, X., Wang, H., & Zhao, H. (2018). Quantitative influence of coast effect on geomagnetically induced currents in power grids: a case study. *J. Space Weather Space Clim*, *8*, A60. doi: 10.1051/swsc/2018046

Lucas, G. M., Love, J. J., & Kelbert, A. (2018). Calculation of voltages in electric power transmission lines during historic geomagnetic storms: An investigation using realistic Earth impedances. *Space Weather*, *16*(2), 181–195. doi: 10.1002/2017SW001779

Marshalko, E., Kruglyakov, M., Kuvshinov, A., Murphy, B. S., Rastätter, L., Ngwira, C., & Pulkkinen, A. (2020). Exploring the influence of lateral conductivity contrasts on the storm time behavior of the ground electric field in the eastern United States. *Space Weather*, *18*(2), 159–195. doi: 10.1029/2019SW002216

Marshall, R. A., Wang, L., Paskos, G. A., Olivares-Pulido, G., Van Der Walt, T., Ong, C., ... Yoshikawa, A. (2019). Modeling geomagnetically induced currents in Australian power networks using different conductivity models. *Space Weather*, *17*(5), 727–756. doi: 10.1002/2017SW001793

Myllys, M., Viljanen, A., Rui, O. A., & Ohnstad, T. M. (2014). Geomagnetically induced currents in Norway: the northernmost high-voltage power grid in the world. *J. Space Weather Space Clim.*, *4*, A10. doi: 10.1051/swsc/2014007

Nakamura, S., Ebihara, Y., Fujita, S., Goto, T., Yamada, N., Watari, S., & Omura, Y. (2018). Time domain simulation of geomagnetically induced current (GIC) flowing in 500-kv power grid in Japan including a three-dimensional ground inhomogeneity. *Space Weather*, *16*(12), 1946–1959. doi: 10.1029/2018SW002004

Pankratov, O., & Kuvshinov, A. (2016). Applied mathematics in EM studies with special emphasis on an uncertainty quantification and 3-D integral equation modelling. *Surv. Geophys.*, *37*(1), 109–147. doi: 10.1007/s10712-015-9340-4

Pokhrel, S., Nguyen, B., Rodriguez, M., Bernabeu, E., & Simpson, J. J. (2018). A finite difference time domain investigation of electric field enhancements along ocean-continent boundaries during space weather events. *J. Geophys. Res. Space Phys.*, *123*(6), 5033–5046. doi: 10.1029/2017JA024648

Pulkkinen, A., Lindahl, S., Viljanen, A., & Pirjola, R. (2005). Geomagnetic storm of 29–31 October 2003: Geomagnetically induced currents and their relation to problems in the Swedish high-voltage power transmission system. *Space Weather*, *3*(8), S08C03. doi: 10.1029/2004SW000123

Püthe, C., & Kuvshinov, A. (2013). Towards quantitative assessment of the hazard from space weather. Global 3-D modellings of the electric field induced by a realistic geomagnetic storm. *Earth Planets Space*, *65*, 1017–1025. doi: 10.5047/eps.2013.03.003

Püthe, C., Manoj, C., & Kuvshinov, A. (2014). Reproducing electric field observations during magnetic storms by means of rigorous 3-D modelling and distortion matrix co-estimation. *Earth Planets Space*, *66*, 162-171. doi: 10.1186/s40623-014-0162-2

Rastätter, L., Toth, G., Kuznetsova, M. M., & Pulkkinen, A. (2014). CalcDeltaB: An efficient post processing tool to calculate ground-level magnetic perturbations from global magnetosphere simulations. *Space Weather*, *12*, 553–565. doi: 10.1002/2014SW001083

Rosenqvist, L., & Hall, J. O. (2019). Regional 3-D modeling and verification of geomagnetically induced currents in Sweden. *Space Weather*, *17*(1), 27–36. doi: 10.1029/2018SW002084

Sokolova, E. Y., Kozyreva, O. V., Pilipenko, V. A., Sakharov, Y. A., & Epishkin, D. V. (2019). Space-weather-driven geomagnetic- and telluric-field variability in northwestern Russia in correlation with geoelectrical structure and currents induced in electric-power grids. *Izv. Atmos. Ocean. Phys*, *55*, 1639–1658. doi:

10.1134/S000143381911015X
Tanskanen, E. I. (2009). A comprehensive high-throughput analysis of substorms observed by IMAGE magnetometer network: Years 1993–2003 examined. *J. Geophys. Res.*, *114*, A05204. doi: 10.1029/2008JA013682
Toffoletto, F., Sazykin, S., Spiro, R., & Wolf, R. (2003). Inner magnetospheric modeling with the Rice Convection Model. In C. A. C.-L. et al. (Ed.), *Advances in space environment research* (pp. 175–196). Springer, Dordrecht. doi: 10.1007/978-94-007-1069-6_19
Toth, G., Sokolov, I., Gombosi, T. I., Chesney, D. R., Clauer, C. R., De Zeeuw, D. L., ... Kota, J. (2005). Space Weather Modeling Framework: A new tool for the space science community. *J. Geophys. Res. Space Phys.*, *110*, A12226. doi: 10.1029/2005JA011126
Toth, G., van der Holst, B., Sokolov, I. V., De Zeeuw, D. L., Gombosi, T. I., Fang, F., ... Opher, M. (2012). Adaptive numerical algorithms in space weather modeling. *J. Comput. Phys.*, *231*(3), 870–903. doi: 10.1016/j.jcp.2011.02.006
van de Kamp, M. (2013). Harmonic quiet-day curves as magnetometer baselines for ionospheric current analyses. *Geosci. Instrum. Method. Data Syst.*, *2*, 289–304. doi: 10.5194/gi-2-289-2013
Vanhamäki, H., & Juusola, L. (2020). Introduction to Spherical Elementary Current Systems. In M. W. Dunlop & H. Lühr (Eds.), *Ionospheric multi-spacecraft analysis tools: Approaches for deriving ionospheric parameters* (pp. 5–33). Cham: Springer International Publishing. doi: 10.1007/978-3-030-26732-2_2
Viljanen, A., & Pirjola, R. (2017). Influence of spatial variations of the geoelectric field on geomagnetically induced currents. *J. Space Weather Space Clim.*, *7*, A22. doi: 10.1051/swsc/2017024
Viljanen, A., Pirjola, R., Prácser, E., Katkalov, J., & Wik, M. (2014). Geomagnetically induced currents in Europe – Modelled occurrence in a continent-wide power grid. *J. Space Weather Space Clim.*, *4*, A09. doi: 10.1051/swsc/2014006
Viljanen, A., Pirjola, R., Prácser, E., Ahmadzai, S., & Singh, V. (2013). Geomagnetically induced currents in europe: Characteristics based on a local power grid model. *Space Weather*, *11*(10), 575–584. doi: 10.1002/swe.20098
Viljanen, A., Pirjola, R., Wik, M., Ádám, A., Prácser, E., Sakharov, Y., & Katkalov, J. (2012). Continental scale modelling of geomagnetically induced currents. *J. Space Weather Space Clim.*, *2*, A17. doi: 10.1051/swsc/2012017
Wang, L., Duan, J., Hitchman, A. P., Lewis, A. M., & Jones, W. V. (2020). Modeling geoelectric fields induced by geomagnetic disturbances in 3D subsurface geology, an example from southeastern Australia. *J. Geophys. Res. Solid Earth*, *125*(9), e2020JB019843. doi: 10.1029/2020JB019843
Wang, L., Lewis, A. M., Ogawa, Y., Jones, W. V., & Costelloe, M. T. (2016). Modeling geomagnetic induction hazards using a 3-D electrical conductivity model of Australia. *Space Weather*, *14*, 1125–1135. doi: 10.1002/2016SW001436
Zhang, B., Sorathia, K. A., Lyon, J. G., Merkin, V. G., Garretson, J. S., & Wiltberger, M. (2019). GAMERA: A three-dimensional finite-volume MHD solver for non-orthogonal curvilinear geometries. *The Astrophysical Journal Supplement Series*, *244*(1), 20. doi: 10.3847/1538-4365/ab3a4c

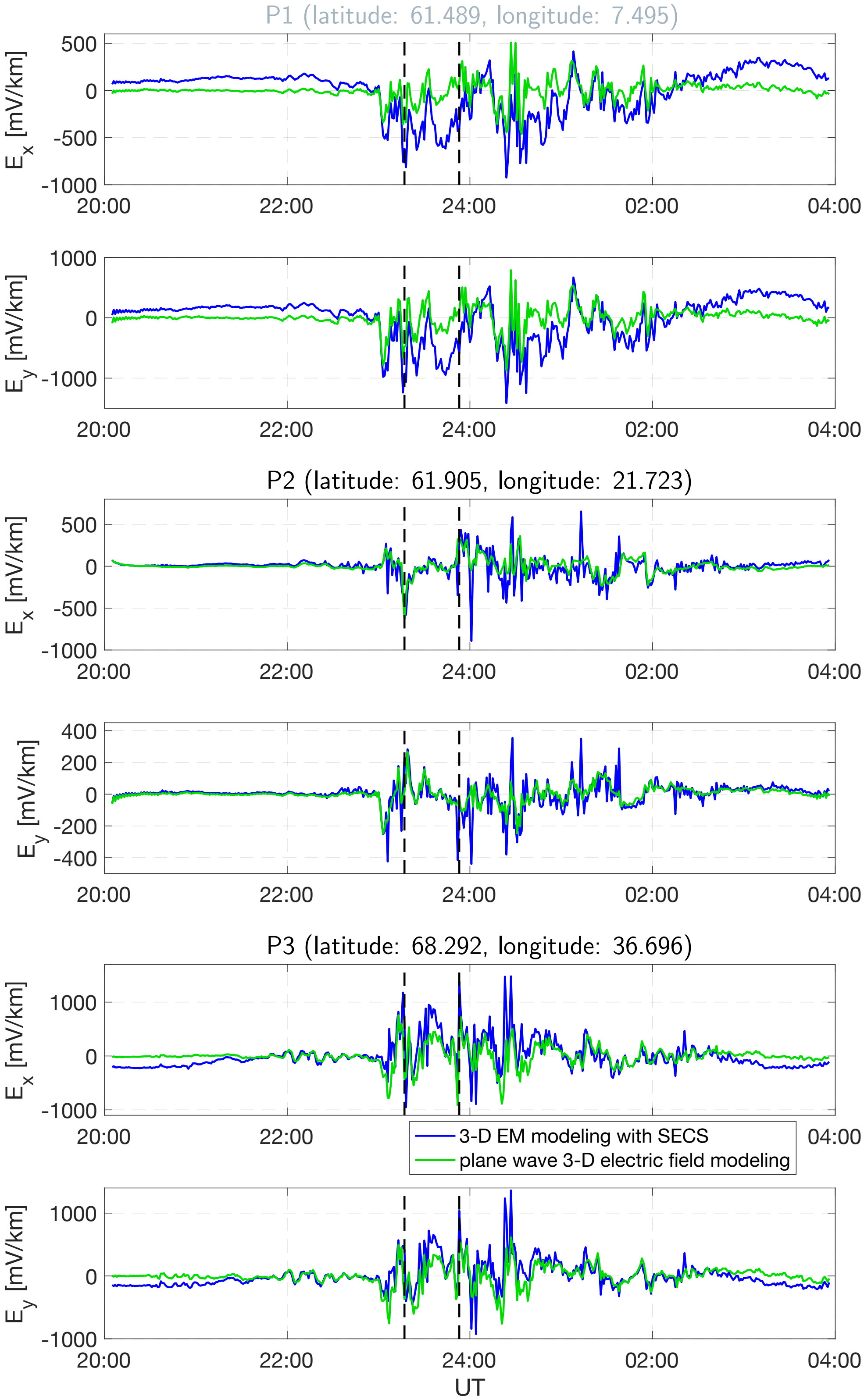

Figure 7. SECS- and plane-wave-based GEF modeling results at three "sites" located in the regions with high lateral conductivity contrasts; locations of these sites are shown in Figure 1.

Figure 8. Top and middle: magnitudes of respective SECS- and MHD-based GEF. Bottom: absolute di erences between corresponding GEF magnitudes.